



OPEN

SUBJECT AREAS:

QUANTUM DOTS

QUANTUM INFORMATION

FLUORESCENCE SPECTROMETRY

NEAR-INFRARED SPECTROSCOPY

Single-photon property characterization of 1.3 μm emissions from InAs/GaAs quantum dots using silicon avalanche photodiodes

P. Y. Zhou, X. M. Dou, X. F. Wu, K. Ding, M. F. Li, H. Q. Ni, Z. C. Niu, D. S. Jiang & B. Q. Sun

State Key Laboratory of Superlattices and Microstructures, Institute of Semiconductors, Chinese Academy of Sciences, P.O. Box 912, Beijing 100083, China.

Received
8 October 2013Accepted
13 December 2013Published
10 January 2014Correspondence and
requests for materials
should be addressed to
B.Q.S. (bqsun@semi.
ac.cn)

We developed a new approach to test the single-photon emissions of semiconductor quantum dots (QDs) in the optical communication band. A diamond-anvil cell pressure device was used for blue-shifting the 1.3 μm emissions of InAs/GaAs QDs to 0.9 μm for detection by silicon avalanche photodiodes. The obtained $g^{(2)}(0)$ values from the second-order autocorrelation function measurements of several QD emissions at 6.58 GPa were less than 0.3, indicating that this approach provides a convenient and efficient method of characterizing 1.3 μm single-photon source based on semiconductor materials.

As an excellent single-photon source, single self-assembled semiconductor quantum dots (QDs) with emissions in the optical communication band, i.e. from 1.3 to 1.5 μm , are attractive candidates for the future fiber-based applications of quantum communication^{1–8}. Single-photon sources can only be statistically confirmed from the anti-bunching measurement of their luminescence², and the results largely depend on the testing setups, especially the performance of the single-photon detectors used. However, as a major single-photon detector employed in the near-infrared spectral range, commercial Peltier-cooled InGaAs avalanche photodiode (APD) has a much higher dark count rate and lower quantum efficiency than silicon APD^{2,3}, which makes it difficult to study 1.3–1.5 μm single-photon sources and obtain exact $g^{(2)}(0)$ value. To solve the single-photon detecting problem in the optical communication band, many researchers have proposed meaningful solutions. To our knowledge, these attempts can be classified into the following three categories: (1) creating micro-structures (such as micro mesas or micro pillars) around single QDs to enhance the collection of their luminescence to offset the low detection efficiency of InGaAs APDs and to improve the signal-to-noise ratio (SNR)^{2,4–8}; (2) using superconducting single-photon detectors (SSPDs)^{3,9–12}, which have higher detection efficiencies and much lower dark count rates than InGaAs APDs¹⁰ and (3) converting the emissions of QDs from the near-infrared range to the visible range, to permit the emissions to be directly detected by more powerful silicon APDs based on the periodically poled LiNbO₃ (PPLN) waveguide quantum frequency up-conversion (QFUC) technology^{3,13–17}. Although these methods have successfully permitted the characterization of semiconductor single-photon sources and obtained credible results, several problems remain in terms of practical use. The micro fabrication of semiconductor QD samples can be cumbersome, which requires subtle fabricating equipment and processing technology. The SSPDs can be costly and require cryogenic operation environment^{3,10}. For the QFUC, the key problem is that a PPLN waveguide with fine structure is not easy to obtain. In addition, a certain PPLN always corresponds to certain conversion frequencies¹³, which make it less flexible in detecting different wavelength emissions from single QDs. Consequently, there are still many areas require improvement in the detection of near-infrared single-photon sources and to make the process more convenient and efficient.

Here, we present a new approach to perform anti-bunching measurements of the optical communication band emissions from semiconductor QDs using both a diamond-anvil cell (DAC) and silicon APDs. InAs/GaAs QDs are used as single-photon sources with 1.3 μm emissions at 0 GPa. Their emissions are successfully shifted from 1.3 to 0.9 μm under high pressure and detected by silicon APDs. The measured $g^{(2)}(0)$ values are less than 0.3 for single QD emissions. The measurement technique is demonstrated to be an effective detection and characterization approach for optical communication band semiconductor non-classical light sources.



Results

The studied InAs/GaAs QD samples with 1.3 μm emissions and various dot densities were all obtained from a wafer grown using the molecular-beam epitaxy method, see Methods for details. Fig. 1b shows the DAC pressure device used for blue-shifting the QD photoluminescence (PL). Condensed argon was used as the pressure-transmitting medium in the DAC. The quasi-hydrostatic pressure can be adjusted at room temperature by driving screws and can be determined *in situ* using the ruby R_1 fluorescence line shift^{18,19}. Fig. 1a presents a schematic diagram of our experimental setup: the QD sample in the DAC was cooled to 4 K using a cryostat of Montana Instruments and excited by a pulsed diode laser at a wavelength of 640 nm, a pulse width of 63 ps and a maximum repetition frequency of 80 MHz. The excitation laser was focused to a ~ 2 μm spot on the sample using a microscope objective (NA: 0.5). The PL was collected using the same objective and separated from the pumping laser using a dichroic mirror and a long pass filter. To accurately detect the PL in various spectral ranges, the longer (> 1 μm) or shorter (< 1 μm) wavelength PL was switched to a 0.3-m focal length monochromator equipped with a liquid-nitrogen-cooled InGaAs linear photodiode array (PDA) or a 0.5-m focal length monochromator equipped with a Peltier-cooled silicon charge-coupled device (CCD), respectively, using a movable mirror. For second-order autocorrelation function $g^{(2)}(\tau)$ measurements of emissions from the QDs at high pressure, a standard Hanbury-Brown and Twiss (HBT) setup²⁰ equipped with two silicon APDs (SPCM-AQR-14: detection efficiency at 0.9 μm $\sim 35\%$ and dark counts ~ 100 cps) and a time-correlated single-photon counting (TCSPC) board were used. The high-pressure PL decay measurements were also performed with the pulsed diode laser and the TCSPC. The PL decay and $g^{(2)}(\tau)$ of a InAs/GaAs QD with a 1.3 μm emission line at 0 GPa were measured by a similar system equipped with two InGaAs APDs (id 201 of ID Quantique).

Fig. 2a–e present the micro-PL spectra from 5 different locations on the QD sample with low dot densities, which exhibit typical spectroscopic fingerprints of single QD emissions. Resolution-limited sharp emission lines can be observed from 1305 to 1335 nm, one of which is perfectly coincident with the minimum loss wavelength of 1310 nm (indicated by the dashed line) in the O-band (1260–1360 nm) of the optical fiber.

Note that the luminescence of InAs/GaAs QDs can be blue-shifted by applying high pressure due to the increase of the Γ -point band-gap^{21–25}. First, we should verify that our method is feasible, and determine which pressure values are suitable for the subsequent PL decay and $g^{(2)}(\tau)$ measurements by silicon APDs. Under certain pressures, due to the mismatch of the QD emission wavelength to the cavity mode (centered at 1320 nm) and the lower detecting ability of the InGaAs PDA (used here to detect PL wavelengths longer than 1 μm), the shifted PL of single QDs often became too weak to detect. Therefore, we selected a location on the QD sample with higher dot density and observed the luminescence evolution of QD ensemble along with the increasing pressure. Fig. 2f summarizes the pressure dependence of the PL peak energy of the QD ensemble. The upper inset clearly reveals that the PL emission peak (1320 nm) at 0 GPa. In the lower inset, the PL peak was almost shifted to 900 nm at 6.52 GPa, where the QD emissions would be more easily detected by silicon APDs (the other detailed spectra under different pressures between 0 and 6.52 GPa are shown in the Supplementary Information, Fig. S1). Note that no other obvious luminescence peaks were observed at wavelengths longer than 940 nm at 6.52 GPa. The solid red line in Fig. 2f represents the result of a linear fit to the experimental data, and the obtained pressure coefficient is 62 meV/GPa. It is consistent with the reported value of 65 meV/GPa for ~ 1240 nm ensemble InAs/GaAs QDs emissions²³. It sounds better if we could apply further pressure to the sample and shift its luminescence to an even shorter wavelength range corresponding to the maximum

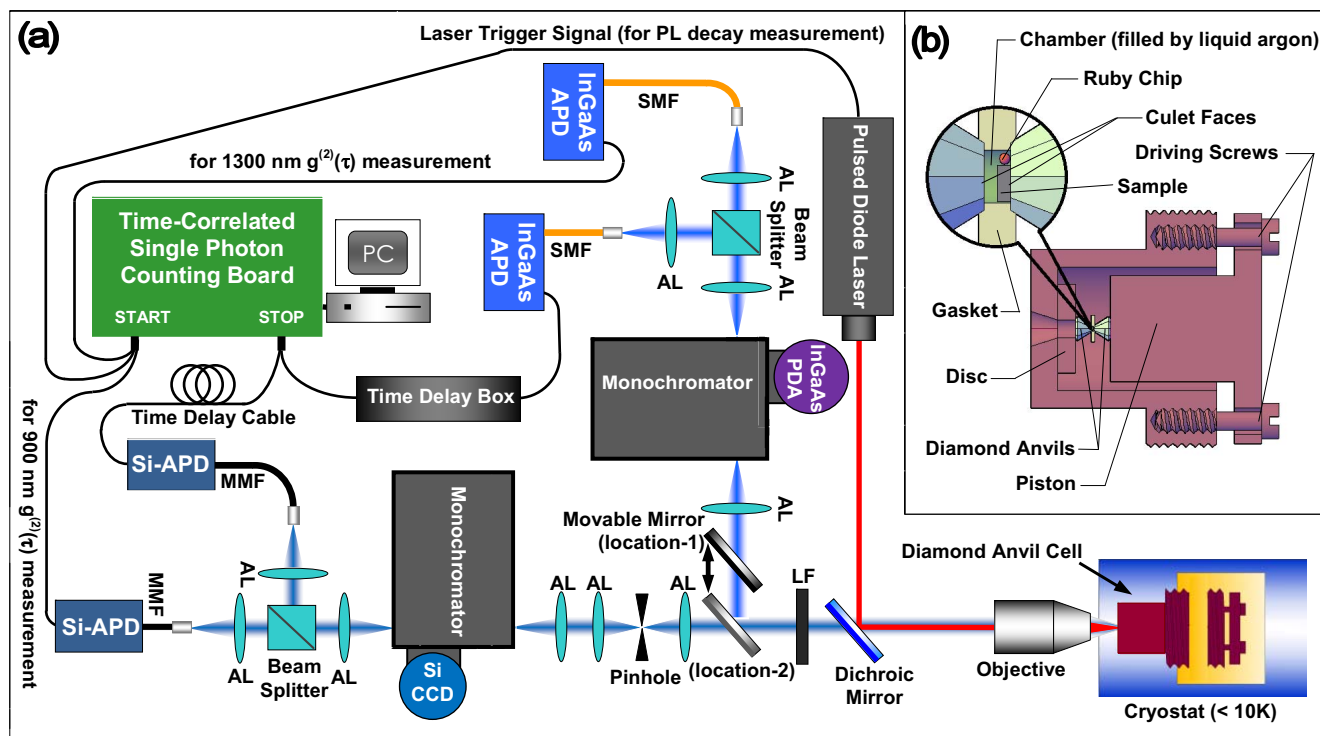


Figure 1 | Schematic of experimental setup and details of high pressure device. (a) Sketch of the experimental setup for time-resolved PL and second-order autocorrelation function measurements under hydrostatic pressure (AL: aspheric lens, APD: avalanche photodiode, CCD: charge-coupled device, PDA: linear photodiode array, LF: long pass filter, SMF: single mode fiber and MMF: multimode fiber). (b) A cross-sectional view of the DAC pressure device used in the experiment.

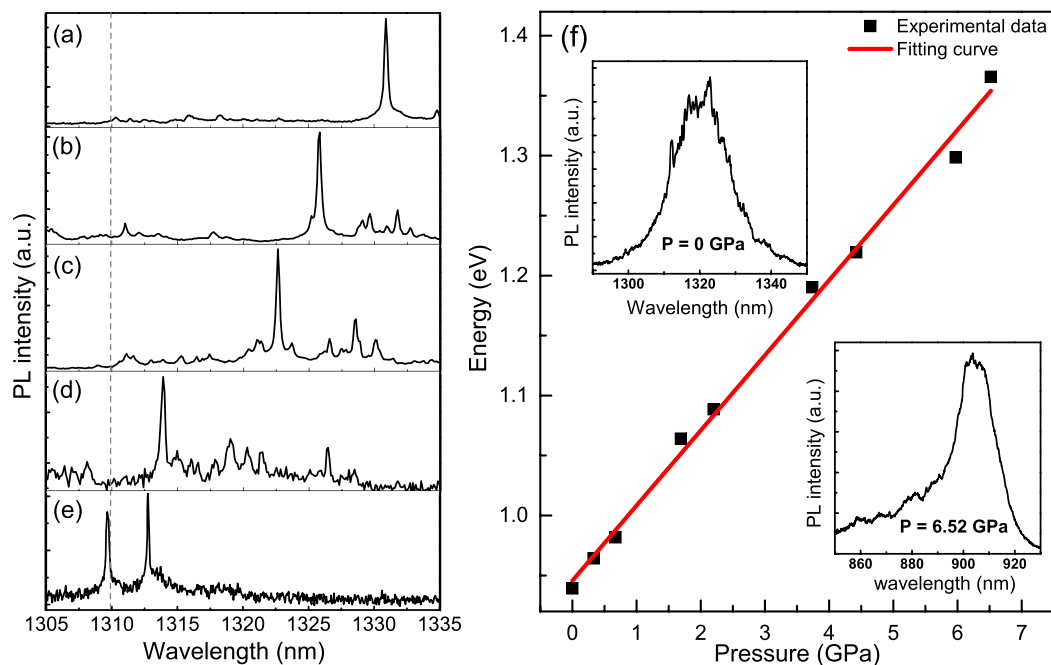


Figure 2 | Photoluminescence spectra of single InAs QDs at 0 GPa and evolution of photoluminescence peak position of ensemble InAs QDs via hydrostatic pressure. (a)–(e) Different emission lines of low-temperature PL from different locations on InAs/GaAs single QD samples at 0 GPa. (f) PL peak energy of InAs/GaAs QD ensemble as a function of pressure (black squares: experimental data; red line: linear fit). The two insets are PL spectra of QD ensemble at 0 and 6.52 GPa.

detection efficiency of silicon APDs ($\sim 65\%$ at 700 nm). However, the PL intensity dropped significantly as the pressure was increased above 7 GPa, mainly due to the zincblende to rocksalt transition (occurs between 7 and 8 GPa) for bulk InAs²³.

Note that the uniaxial or biaxial stress generated by an integrated piezoelectric unit can be another effective approach to tune the emissions of the semiconductor QDs^{21,22,25–28}, whereas the limited spectral tuning range (the largest one is ~ 8 nm^{27,28}) would not meet the demand of a large wavelength shift for this work.

A QD sample with 1.3 μm emissions as shown in Fig. 2a–e was selected to be placed into the DAC chamber, and a pressure of 6.58 GPa was applied at 4 K. Single QD emission lines from the sample are shown in the left panels of Fig. 3a–c. Time-resolved PL spectra of the 901.5, 896.6, 883.2 and 882.6 nm emission lines are shown on the upper right side of Fig. 3a–c. The lifetimes obtained by single-exponential fits after deconvolution with the measured TCSPC (equipped with silicon APDs) setup response function (SRF, see Supplementary Information, Fig. S2) were 1.27, 1.10, 1.36 and 1.05 ns, respectively, which are typical values for the radiative lifetimes of exciton recombination in InAs/GaAs QDs. However, the external pressure would change the Coulomb Integral J_{eh} and thus influences the dipole strength and radiative lifetime. To figure out the evolution of QD luminescence lifetime with pressure, we measured two InAs/GaAs QDs (with emissions of ~ 0.9 μm at 0 GPa and the QD sample without top and bottom DBRs) PL decay curves at different pressures from 0 to 3.25 GPa. The results show that the lifetimes slightly decrease with increasing pressure (see Supplementary Information, Fig. S3).

The $g^{(2)}(\tau)$ for these emission lines from QDs at 6.58 GPa were measured using an HBT setup equipped with silicon APDs, as described in Fig. 1. In the experiments, single QDs (detected by silicon CCD) with an average count rate larger than 3000 cps were selected for the $g^{(2)}(\tau)$ measurements and each integration time was 2 h. The obtained autocorrelation histograms are shown, respectively, in the lower right panels of Fig. 3a–c as black lines. The strong suppression of correlation peaks at zero time delay provides evidence

of the anti-bunching behavior of the quantum light emission from these QDs. To obtain the exact values of $g^{(2)}(0)$, we fit the experimental data using a formula for non-resonant pulsed excitation²⁹:

$$N^{-1} \left\{ B + \sum_n \alpha_n \exp \left(- \frac{|\tau - n \cdot T_{\text{rep}}|}{\tau_e} \right) \right\} \quad (1)$$

where N , B , τ_e , α_n and T_{rep} are the normalization factor, baseline value, lifetime of the emitter, correlation peak height of the n th excitation cycle ($0 \leq \alpha_n \leq 1$, $\alpha_{n \neq 0} \sim 1$), and repetition period of the excitation pulses, respectively. The fitting results are displayed as red-solid lines in Fig. 3, and all the $g^{(2)}(0)$ values are less than 0.3.

We also have directly measured the PL decay and $g^{(2)}(\tau)$ of a single QD at 0 GPa with InGaAs APDs for comparison. To facilitate the measurements, we selected a single emission line with the highest PL intensity (~ 8000 cps, as measured by the InGaAs PDA under saturated excitation by the diode laser with a repetition frequency of 80 MHz) from the ones we strived to find around the cavity mode of 1320 nm as shown in Fig. 4a. Based on the parameter settings of InGaAs APDs in Reference (8), we measured the PL decay of the single QD under 1 MHz laser excitation. The lifetime 1.23 ns of the 1331.9 nm line, obtained by single-exponential fits to the PL decay data after deconvolution with the SRF (see Supplementary Information, Fig. S4) of the TCSPC equipped with InGaAs APDs, which is consistent with the reported values^{4,5,8}. For $g^{(2)}(\tau)$ measurements, a laser repetition frequency of 2 MHz was selected, and the excitation power was adjusted to attain the best SNR. The InGaAs APDs worked in a gated mode with a 5-ns gate time and were well synchronized with the trigger signal from the diode laser. The detection efficiency of the APDs was set to 15%. Two different detection results were obtained by setting the dead time of the InGaAs APDs to 1 and 10 μs , respectively, with the accumulation time being set to 10 h. Fig. 4c and d demonstrate that even $g^{(2)}(\tau)$ has a clear anti-bunching dip, and the obtained $g^{(2)}(0)$ values are relatively large at 0.63 ± 0.04 and 0.51 ± 0.05 , respectively (the raw data and background of the $g^{(2)}(\tau)$ measurements can be found in Supplementary Information, Fig. S5).

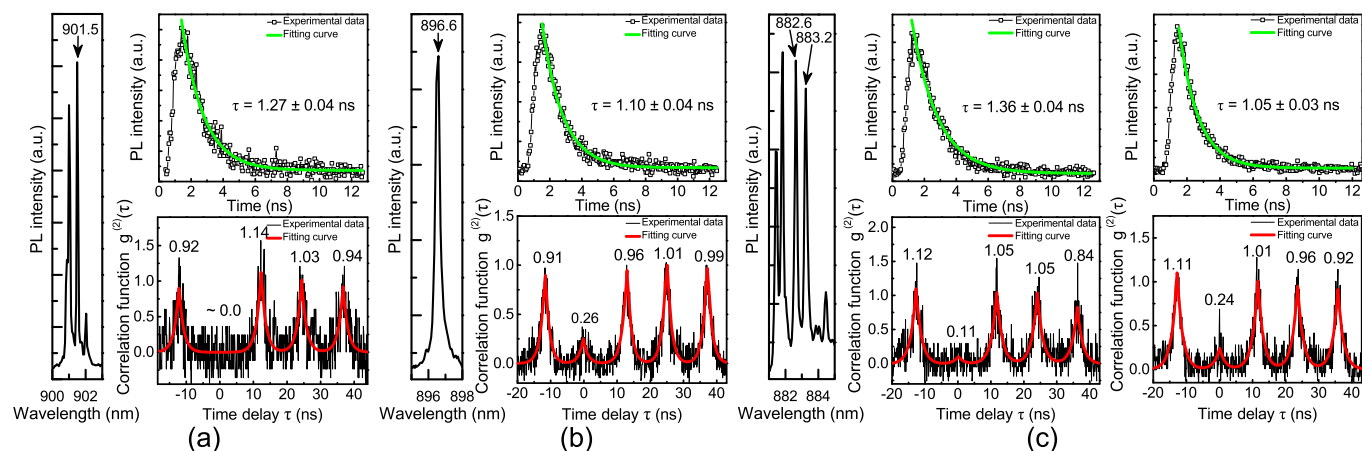


Figure 3 | Photoluminescence spectra, time-resolved spectra and single photon emissions of single InAs QDs at high pressure. (a)–(c) Several emission lines of low temperature PL that were observed from the different locations on the sample at 6.58 GPa (left panels), their PL intensity decay curves (upper right panels), and their second-order autocorrelation function measurements (lower right panels).

Note that the relatively large-dark counts and the after-pulses of InGaAs APDs may lead to higher $g^{(2)}(0)$ values. To attain better results, a shorter gate time, lower detection efficiency, longer dead time and smaller excitation repetition frequency would be ideal. However, these settings may also cause the loss of some useful counts, and the measurements would be time consuming. Compared with the inherent dark counts of InGaAs APDs, the after-pulse effect may be more harmful to the $g^{(2)}(\tau)$ measurements because the effect of dark counts can be statistically removed by background subtraction; however, the after-pulses can confuse the noise with useful signals and thus cause them to be not well separated. By selecting a longer dead time 10 μs instead of 1 μs , the obtained $g^{(2)}(0)$ value decreases from 0.63 ± 0.04 to 0.51 ± 0.05 , indicating that the after-pulse effect of the InGaAs APDs is really an

important factor for altering the $g^{(2)}(\tau)$ measurements. Unfortunately, too long of a dead time could not be selected for real measurements. The use of a tunable band pass filter and the creation of a micro-structure around a single QD were also reported to enhance the collection efficiency and SNR of $g^{(2)}(\tau)$ measurements^{2,4–8}. However, the $g^{(2)}(\tau)$ measurement proposed using DAC and more powerful silicon APDs was demonstrated to be a more effective approach to characterize the single-photon emission of QDs at 1.3 μm . In fact, it will also be possible to extend this method to characterize QDs with single-photon emissions at 1.55 μm .

Finally, to further confirm the feasibility of the proposed approach, we traced the $g^{(2)}(\tau)$ evolution of a single QD (with a emission line of ~ 900 nm at 0 GPa) under pressure from 0 to 3 GPa, herein the $g^{(2)}(\tau)$ was measured using silicon APDs. The

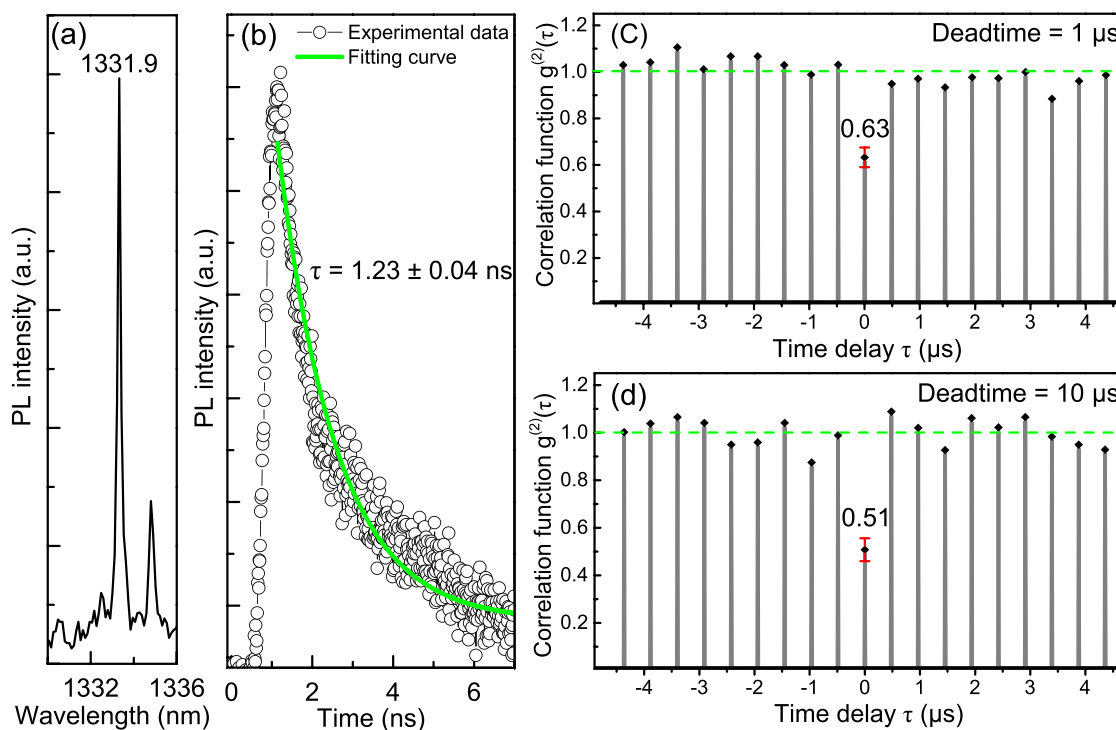


Figure 4 | Photoluminescence spectrum, time-resolved spectrum and single-photon characterization of a InAs QD at 0 GPa. (a) PL emission line of a single InAs/GaAs QD at 0 GPa. (b) PL intensity decay curve of emission line in (a). Second-order autocorrelation function measurements of the QD emission by InGaAs APDs with dead times of 1 μs (c) and 10 μs (d) (the error bars are obtained from the mean square errors of correlation peak heights without the one at zero time delay).



results indicate that the single-photon emission mechanism of the QD remains well under different pressures (see Supplementary Information, Fig. S6). In addition, it was found that the tuned QD emission line is reversible as a function of pressure.

Discussion

In summary, we have introduced a new approach that can efficiently characterize the single-photon emission property of semiconductor QDs with wavelength in the optical communication band at 0 GPa. By combining a DAC and a micro PL system, we have obtained a pressure coefficient of 62 meV/GPa for 1.3 μm ensemble InAs/GaAs QDs, and determined the suitable pressure range ($\sim 6.5\text{--}7.0$ GPa) for $g^{(2)}(\tau)$ measurements of luminescence from single QDs. By applying quasi-hydrostatic pressure on single InAs/GaAs QDs, we successfully shifted their emission lines from 1.3 μm (at 0 GPa) to ~ 0.9 μm (at 6.58 GPa). The second-order autocorrelation function of the emission lines from single QDs could be better measured at high pressure by silicon APDs, and the obtained results ($g^{(2)}(0) < 0.3$) confirmed that these single QDs correspond to single-photon sources in the 1.3 μm range at 0 GPa. Through a comparison with the conventional anti-bunching measurements of a 1.3 μm emission line from an InAs/GaAs QD at 0 GPa by InGaAs APDs, the advantage of the new approach is demonstrated.

Note that the effect of quasi-hydrostatic pressure on the QD sample is mainly to enlarge the band-gap energy, i.e., to blue-shift the PL peak energy. Moreover, for bulk GaAs, the energy of the direct Γ point band gap increases with pressure while the energy of the X-like minimum is lowered, leading to a direct to indirect band gap cross-over at about 4.2 GPa²⁵. Then the QD luminescence intensity will decrease with a further increasing pressure due to the fact that the capture ability of QDs for the carriers (generated by laser) from GaAs host material decreases after GaAs becomes an indirect band semiconductor^{23–25}. It would be a drawback for the detection of QD emissions at high pressure. However, based on the experimental results reported here and in References (24) and (25), we argue that the pressure-induced luminescence quenching effect can be weakened for large dots. Therefore, we consider that the method proposed here can be helpful for characterizing the single-photon properties of QDs with emissions in the optical communication band using more reliable silicon APDs.

Methods

Samples preparation. The studied InAs QD samples with 1.3 μm emissions and various dot densities were all obtained from a wafer grown using the molecular-beam epitaxy method on a (001) GaAs substrate. In detail, they consist of, in sequence, a 200 nm GaAs buffer layer, a 20-period GaAs/AlAs (each $\lambda/4$ period consists of a 96.06 nm thick GaAs layer and a 112.8 nm thick AlAs layer) distributed Bragg reflector (DBR), a layer of 96.06 nm GaAs, a 2.42 monolayers (ML) of InAs, a layer of 8 nm GaAs, a QD layer with 1.3 μm emission and various dot densities formed by nominal 2 ML of InAs (during the QD layer growth, GaAs substrate stops running in order to obtain various QD density distributions) and capped by a 5 nm $\text{In}_{0.15}\text{Ga}_{0.85}\text{As}$ strain-reducing layer followed by a 192.12 nm GaAs layer and a 4-period GaAs/AlAs DBR with the same period as the bottom. To fit the QD samples into the diamond-anvil cell chamber, the samples were mechanically thinned to a thickness of approximately 20 μm and then cut into pieces approximately $100 \times 100 \mu\text{m}^2$ in size.

Calibration of the ruby pressure gauge under quasi-hydrostatic condition. The values of quasi-hydrostatic pressure applied to QD samples were determined in situ using the ruby R_1 fluorescence line shift^{18,19}. For our experiment, concentrate pressure values were calculated by the followed equation:

$$P = \frac{1904}{B} \times \left[\left(\frac{\lambda}{\lambda_0} \right)^B - 1 \right] \quad (2)$$

where P is the pressure in GPa, λ_0 is the wavelength of ruby R_1 at zero pressure and λ is the wavelength of the ruby R_1 line at some certain pressure which want to be known, B is a constant with the value 7.665.

1. Yuan, Z. *et al.* Electrically Driven Single-Photon Source. *Science* **295**, 102–105 (2002).

2. Takemoto, K. *et al.* Non-classical photon emission from a single InAs/InP quantum dot in the 1.3- μm optical-fiber band. *Jpn. J. Appl. Phys.* **43**, L993–L995 (2004).
3. Eisaman, M. D., Fan, J., Migdall, A. & Polyakov, S. V. Single-photon sources and detectors. *Rev. Sci. Instrum.* **82**, 071101 (2011).
4. Xu, X. L. *et al.* “Plug and Play” single photons at 1.3 μm approaching gigahertz operation. *Appl. Phys. Lett.* **93**, 021124 (2008).
5. Ward, M. B. *et al.* Electrically driven telecommunication wavelength single-photon source. *Appl. Phys. Lett.* **90**, 063512 (2007).
6. Ward, M. B. *et al.* On-demand single-photon source for 1.3 μm telecom fiber. *Appl. Phys. Lett.* **86**, 201111 (2005).
7. Usuki, T. *et al.* Single-photon generator for optical telecommunication wavelength. *J. Phys.: Conf. Ser.* **38**, 140–143 (2006).
8. Zinoni, C. *et al.* Time-resolved and antibunching experiments on single quantum dots at 1300 nm. *Appl. Phys. Lett.* **88**, 131102 (2006).
9. Elvira, D. *et al.* Single InAs_{1-x}P_x/InP quantum dots as telecommunications-band photon sources. *Phys. Rev. B* **84**, 195302 (2011).
10. Natarajan, C. M., Tanner, M. G. & Hadfield, R. H. Superconducting nanowire single-photon detectors: physics and applications. *Supercond. Sci. Technol.* **25**, 063001 (2012).
11. Elvira, D. *et al.* Time-resolved spectroscopy of InAsP/InP(001) quantum dots emitting near 2 μm . *Appl. Phys. Lett.* **97**, 131907 (2010).
12. Zaske, S. *et al.* Visible-to-telecom quantum frequency conversion of light from a single quantum emitter. *Phys. Rev. Lett.* **109**, 147404 (2012).
13. Ma, L. J., Slattery, O. & Tang, X. Single photon frequency up-conversion and its applications. *Phys. Rep.* **521**, 69–94 (2012).
14. Albota, M. A. & Wong, F. N. C. Efficient single-photon counting at 1.55 μm by means of frequency upconversion. *Opt. Lett.* **29**, 1449–1451 (2004).
15. Vandevender, A. P. & Kwiat, P. G. High efficiency single photon detection via frequency up-conversion. *J. Mod. Optic.* **51**, 1433–1445 (2004).
16. Roussev, R. V., Langrock, C., Kurz, J. R. & Fejer, M. M. Periodically poled lithium niobate waveguide sum-frequency generator for efficient single-photon detection at communication wavelengths. *Opt. Lett.* **29**, 1518–1520 (2004).
17. Rakher, M. T., Ma, L., Slattery, O., Tang, X. & Srinivasan, K. Quantum transduction of telecommunications-band single photons from a quantum dot by frequency upconversion. *Nat. Photonics* **4**, 786–791 (2010).
18. Piermarini, G. J., Block, S., Barnett, J. D. & Forman, R. A. Calibration of pressure-dependence of R_1 ruby fluorescence line to 195 kbar. *J. Appl. Phys.* **46**, 2774–2780 (1975).
19. Mao, H. K., Xu, J. & Bell, P. M. Calibration of the ruby pressure gauge to 800-kbar under quasi-hydrostatic conditions. *J. Geophys. Res.* **91**, 4673–4676 (1986).
20. Brown, R. H. & Twiss, R. Q. Question of correlation between photons in coherent light rays. *Nature* **178**, 1447–1448 (1956).
21. Dou, X. M. *et al.* Tuning photoluminescence energy and fine structure splitting in single quantum dots by uniaxial stress. *Chin. Phys. Lett.* **25**, 1120 (2008).
22. Trotta, R. *et al.* Nanomembrane quantum-light-emitting diodes integrated onto piezoelectric actuators. *Adv. Mater.* **24**, 2668–2672 (2012).
23. Manjón, F. J., Goñi, A. R., Syassen, K., Heinrichsdorff, F. & Thomsen, C. Pressure dependence of photoluminescence spectra of self-assembled InAs/GaAs quantum dots. *Hys. Stat. Sol. (b)* **235**, 496–500 (2003).
24. Ma, B. S. *et al.* Photoluminescence from self-assembled long-wavelength InAs/GaAs quantum dots under pressure. *J. Appl. Phys.* **95**, 933–938 (2004).
25. Li, G. H., Goni, A. R., Abraham, C., Syassen, K. & Santos, P. V. Photoluminescence from strained InAs monolayers in GaAs under pressure. *Phys. Rev. B* **50**, 1575–1581 (1994).
26. Seidl, S. *et al.* Effect of uniaxial stress on excitons in a self-assembled quantum dot. *Appl. Phys. Lett.* **88**, 203113 (2006).
27. Ding, F. *et al.* Tuning the Exciton Binding Energies in Single Self-Assembled InGaAs/GaAs Quantum Dots by Piezoelectric-Induced Biaxial Stress. *Phys. Rev. Lett.* **104**, 067405 (2010).
28. Rastelli, A. *et al.* Controlling quantum dot emission by integration of semiconductor nanomembranes onto piezoelectric actuators. *Phys. status solidi (b)* **249**, 687–696 (2012).
29. Nakajima, H., Kumano, H., Iijima, H. & Suemune, I. Anomalous dip observed in intensity autocorrelation function as an inherent nature of single-photon emitters. *Appl. Phys. Lett.* **101**, 161107 (2012).

Acknowledgments

This work is supported by the National Key Basic Research Program of China (Grant Nos. 2013CB922304, 2013CB933304), the National Natural Science Foundation of China (Grant No. 90921015) and the Strategic Priority Research Program (B) of the Chinese Academy of Sciences (Grant No. XDB01010200).

Author contributions

P.Y.Z., B.Q.S. and D.S.J. wrote the main manuscript text. M.F.L., H.Q.N. and Z.C.N. grew the quantum dot material. P.Y.Z., X.M.D. and B.Q.S. performed the measurements, in part using a diamond-anvil cell pressure device developed by K.D. and X.F.W. All authors reviewed the manuscript.



Additional information

Supplementary information accompanies this paper at <http://www.nature.com/scientificreports>

Competing financial interests: The authors declare no competing financial interests.

How to cite this article: Zhou, P.Y. *et al.* Single-photon property characterization of 1.3 μm

emissions from InAs/GaAs quantum dots using silicon avalanche photodiodes. *Sci. Rep.* **4**, 3633; DOI:10.1038/srep03633 (2014).



This work is licensed under a Creative Commons Attribution-NonCommercial-NoDerivs 3.0 Unported license. To view a copy of this license, visit <http://creativecommons.org/licenses/by-nc-nd/3.0>